

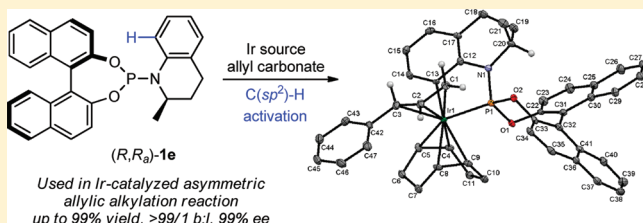
Iridium-Catalyzed Allylic Alkylation Reaction with N-Aryl Phosphoramidite Ligands: Scope and Mechanistic Studies

Wen-Bo Liu, Chao Zheng, Chun-Xiang Zhuo, Li-Xin Dai, and Shu-Li You*

State Key Laboratory of Organometallic Chemistry, Shanghai Institute of Organic Chemistry, Chinese Academy of Sciences, 345 Lingling Lu, Shanghai 200032, People's Republic of China

S Supporting Information

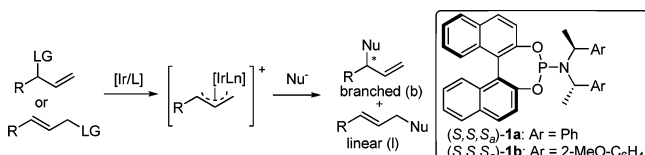
ABSTRACT: A series of N-aryl phosphoramidite ligands has been synthesized and applied to iridium-catalyzed allylic alkylation reactions, offering high regio- and enantioselectivities for a wide variety of substrates. These ligands feature the synthetic convenience and good tolerance of the ortho-substituted cinnamyl carbonates. Mechanistic studies, including DFT calculations and X-ray crystallographic analyses of the (π -allyl)-Ir complexes, reveal that the active iridacycle is formed via C(sp²)-H bond activation.



INTRODUCTION

During the past decade significant progress has been made in the field of iridium-catalyzed allylic substitution reactions, which has been developed into a reliable method to construct chiral centers in organic synthesis.^{1,2} The reaction allows the preparation of highly enantioenriched allylic compounds from readily available monosubstituted allylic substrates (Scheme 1).

Scheme 1. Ir-Catalyzed Allylic Substitution Reactions



Since the first report on iridium-catalyzed asymmetric allylic alkylation reactions with oxazolinyl-phosphine ligands,³ many catalytic systems involving chiral ligands⁴ such as binaphthol-based phosphoramidites,^{4a–h} diene ligands,⁴ⁱ phosphoramidite–olefin ligands,^{4j,k} and others^{4l–n} have been developed to afford excellent levels of regio- and enantioselectivity.

In particular, the Feringa-type ligand **1a**,⁵ first employed in Ir-catalyzed allylic amination by the Hartwig group,^{4b} was used most frequently, providing high regio- and enantioselectivity for various nucleophiles. Then the Alexakis group developed the *o*-methoxy-substituted ligand **1b**,^{4d} which induced higher selectivities in many cases. The mechanistic studies carried out by Hartwig and co-workers disclosed that the active catalytic species of the iridium complex was formed via an insertion of the Ir center into the C(sp³)-H bond in the methyl group of the amine part of the ligand.^{1c,6a} The (π -allyl)-Ir complex intermediates were also synthesized, isolated, and confirmed recently.^{6b,7} Despite the broad substrate scope, with the iridium catalyst derived from ligand **1a** or **1b**, ortho-

substituted cinnamyl substrates in general could not be tolerated, with much decreased enantioselectivities observed for many different types of nucleophiles.^{4b,8,9} A plausible explanation is the steric hindrance between ligands and substrates.^{7b} Recently, we synthesized a series of phosphoramidite ligands from the readily available secondary amines and enantiopure BINOL, which resulted in good regio- and enantioselectivities for a broad range of substrates, including ortho-substituted phenyl allylic substrates.⁹ In addition, these ligands were also found to be effective in the iridium-catalyzed asymmetric intramolecular allylic dearomatization of indoles and pyrroles.¹⁰ DFT calculation and X-ray analyses of crystal structures of the (π -allyl)-Ir intermediates showed that the active catalytic species was formed via C(sp²)-H bond activation of the ligand. Inspired by these results, various phosphoramidite ligands were synthesized to confirm the importance of the N-aryl moiety, accounting for the formation of a catalytic iridacycle. Moreover, these ligands were found to be highly efficient for Ir-catalyzed allylic alkylation reactions. Here, we report the details of this study.

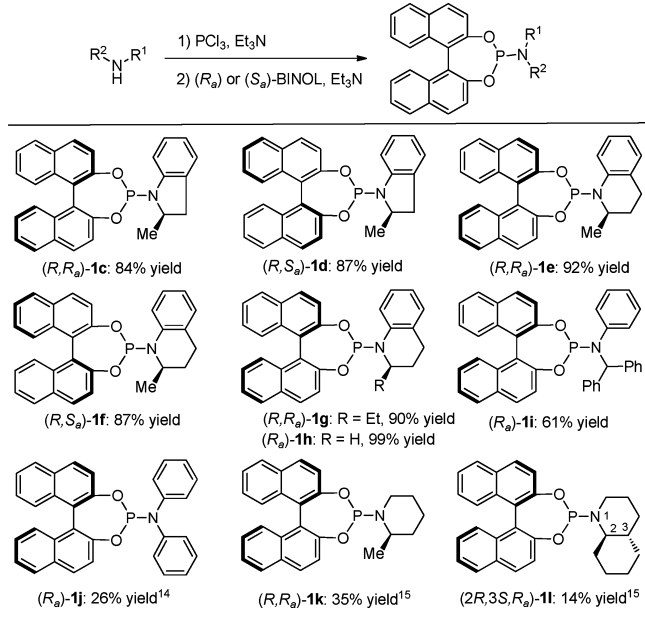
RESULTS AND DISCUSSION

Design and Synthesis of N-Aryl Phosphoramidite Ligands. The initial design of phosphoramidite ligands was focused on binaphthol-based species derived from amines bearing an α -methyl group, imitating the phenethyl amino moiety in the Feringa ligand, as we have thought this is critical to form the active iridacycle catalyst by Ir-mediated C(sp³)-H bond insertion.^{1c} For this purpose, enantiopure 2-methylindoline¹¹ and 2-methyltetrahydroquinoline¹² were chosen as the amine moieties. Phosphoramidite ligands **1c–f** were synthesized in a one-pot procedure (Scheme 2).¹³ After further

Received: November 21, 2011

Published: February 7, 2012

Scheme 2. Synthesis of the Phosphoramidite Ligands



understanding the catalysts derived from these ligands, we realized that the active catalyst might be formed via Ir-mediated C(sp²)–H bond insertion rather than C(sp³)–H bond insertion. Therefore, enantiopure 2-ethyltetrahydroquinoline and several commercially available achiral N-aryl amines were also used, giving phosphoramidite ligands **1g** and **1h–1j**¹⁴ (with only axial chirality). Ligands **1k,l** were prepared by using the racemic amines and (R_{a})-BINOL, and the enantiopure

ligands could be obtained after recrystallization in ethyl acetate.¹⁵ Most of the ligands synthesized above are crystalline solids and can be readily purified.¹⁶

Optimization of Reaction Conditions. To test the suitability of these N-aryl ligands in Ir-catalyzed allylic substitution reactions, we began our study by choosing cinnamyl carbonate and sodium dimethyl malonate as substrates, along with the catalysts derived from [Ir(cod)Cl]₂ and phosphoramidites. The results are summarized in Table 1. Ligands **1c–f** were screened following procedure A, with LiCl as the additive, developed by Helmchen and co-workers.^{4a} The catalysts derived from **1c,d** were ineffective for this reaction, with very low conversion (entries 1 and 2). The reaction with ligand **1e** proceeded in excellent yield, regioselectivity, and enantioselectivity ($3\text{a}/4\text{a} = 97/3$, 97% ee for **3a**, entry 3). Ligand **1f**, a diastereoisomer of **1e**, only led to the formation of the product in 20% yield and 78% ee with reversed absolute configuration (entry 4). Comparison of the results obtained from ligands **1e,f** not only clearly shows the match of two kinds of chiralities in **1e** but also indicates that the enantiocontrol is dominated by the axial chirality of the ligands (entries 3 and 4). Due to the fact that the reaction is much faster with **1e** than with **1f**,^{4f} the diastereomeric mixture of ligands **1e***, prepared from (R_{a})-BINOL and racemic 2-methyltetrahydroquinoline, were also tested in the reaction. As expected, the reaction with **1e*** gave the alkylation product in 92% yield and 92% ee (entry 5).

Different procedures of catalyst preparation and reaction conditions were also investigated. The combination of dry triazabicyclodecene (TBD), tetrahydrothiophene (THT), and CuI (procedure B) was found previously to be very efficient for allylic alkylation reactions, particularly in conjunction with

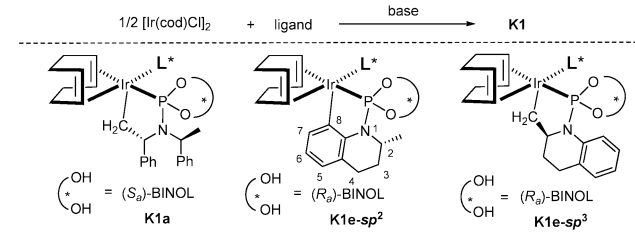
Table 1. Investigation of Ligands in Ir-Catalyzed Allylic Alkylation Reactions^a

entry	ligand	procedure ^b	t (h)	3a/4a ^c	yield (%) ^d	ee (%) ^e
1	1c	A	24	92/8	ND ^f	ND ^f
2	1d	A	24	90/10	16	73 (S)
3	1e	A	5	97/3	91	97 (R)
4	1f	A	24	83/17	20	78 (S)
5	(rac- C,R_{a})- 1e*	A	12	97/3	92	92 (R)
6	1e	B	<1	97/3	94	96 (R)
7 ^{4e}	1a	B	1	99/1	88	96 (R)
8	1e	C	<1	97/3	95	98 (R)
9 ^g	1e	C	12	97/3	96	95 (R)
10	1g	C	2	97/3	95	95 (R)
11	1h	C	12	86/14	95	95 (R)
12	1i	C	12	92/8	42 ^h	92 (R)
13	1j	C	12	94/6	61 ^h	85 (R)
14 ⁱ	1k	C	48	73/27	30 ^h	13 (S)
15 ⁱ	1l	C	48	76/24	49 ^h	10 (S)

^aThe reactions were conducted at room temperature on a 0.25 mmol scale in THF (2.5 mL) with a relative mole ratio **2a**:NaCH(CO₂Me)₂: [Ir(cod)Cl]₂:**1** of 1:2:0.02:0.04. ^bProcedure A: [Ir(cod)Cl]₂ and **1** were stirred in THF for 20 min at room temperature, and then LiCl (100 mol %) and substrates were added. Procedure B: [Ir(cod)Cl]₂, **1**, TBD (12 mol %), and THT (20 mol %) were stirred in THF for 2 h at room temperature, and then CuI (20 mol %) and substrates were added. Procedure C: [Ir(cod)Cl]₂, **1**, and n-PrNH₂ (0.3 mL) were stirred in THF (0.5 mL) for 30 min at 50 °C, and then the volatiles were removed under vacuum to yield the catalyst. See the Supporting Information for details. ^cDetermined by ¹H NMR of the crude reaction mixture. ^dIsolated yield of **3a** and **4a**. ^eDetermined by HPLC analysis; the absolute configuration is indicated in parentheses. ^fNot determined. ^g0.5 mol % [Ir(cod)Cl]₂ and 1 mol % **1e** were used. ^hConversion of **2a**. ⁱ10 mol % [Ir(cod)Cl]₂ and 20 mol % **1** were used.

ligand **1a**.^{4d} Further investigations by Hartwig and co-workers led to procedure C,^{8a} a general method for catalyst preparation using *n*-propylamine to induce the formation of cyclometalated complex **K1a**^{6a} via a C–H bond activation at the methyl group of ligand **1a** (Scheme 3). Procedures B and C could both

Scheme 3. Cyclometalated Ir Complexes



obviously increase the rate of the reaction (entries 6 and 8). The reaction with ligand **1e** proceeded in higher yield and ee than those with Feringa ligand **1a** (entries 7 and 8). Even with a reduced catalyst loading (0.5 mol % of catalyst), the product could be obtained in 96% yield together with 97/3 regioselectivity and 95% ee (entry 9).

Encouraged by these results, we next examined the rest of the phosphoramidite ligands synthesized above. Ligand **1g**, bearing a 2-ethyltetrahydroquinoline moiety, could afford regioselectivity and enantioselectivity (95% ee, entry 10) comparable to those of ligand **1e** under the same reaction conditions (entry 8).

Next, phosphoramidites **1h–j**, containing achiral aromatic amines and (*R*_a)-BINOL as the only stereochemical element, were surveyed. The reaction with **1h** occurred smoothly in excellent yield and ee, indicating that the methyl group β to nitrogen is not necessary for the cyclometalation (entry 11).^{4f} The more steric bulky ligands **1i,j** also afforded the desired product in good regioselectivity and enantioselectivity, with moderate yields (entries 12 and 13). In contrast, ligands **1k,l**, containing chiral aliphatic amines, were screened in the reaction, affording the product in low conversion and enantioselectivity (entries 14 and 15). Notably, the absolute configuration of branched products was reversed in both cases. All the experimental data above suggest that the phenyl group on the nitrogen in the ligands plays an important role in this reaction. It is likely that the cyclometalation of iridium complexes generated from ligands **1c–j** might be formed via C(sp²)–H bond activation instead of C(sp³)–H bond activation observed with the Feringa ligand.

Reaction Scope. With the optimized reaction conditions in hand (2 mol % of $[\text{Ir}(\text{cod})\text{Cl}]_2$, 4 mol % of **1e**, and 200 mol % of $\text{NaCH}(\text{CO}_2\text{Me})_2$ in THF at room temperature), the substrate scope was examined by varying the substituents on the allylic carbonates (Table 2). The results from ligands **1a,b** are also included for comparison.

With ligand **1e**, the reactions of allylic carbonates bearing an electron-donating group (–OMe) at the para- or meta positions of the aromatic ring both gave excellent yields, regioselectivities, and ee (entries 6 and 8, Table 2), almost the same as those obtained from ligands **1a** (entry 4) and **1b** (entries 5 and 7). It should be noted that the stereochemistry of the branched products remains the same, although the binaphthol chirality of (*R*_a)-**1e** is different from that of (*S,S,S*_a)-**1a** and (*S,S,S*_a)-**1b** (entries 1–8).

Table 2. Scope of the Allylic Carbonates^a

entry	$\text{R}, \text{2}$	1	t (h)	$3/4^b$	yield (%) ^c	ee (%) ^d
1 ^{4e}		1a	1	99/1	88	96 (R)
2 ^{8c}		1b	2	99/1	87	98 (R)
3		1e	<1	97/3	95	98 (R)
4 ^{4e}		1a	<1	99/1	95	97 (R)
5 ^{8c}		1b	24	>99/1	99	97 (R)
6		1e	<1	>99/1	96	95 (R)
7 ^{8c}		1b	6	99/1	58	96 (R)
8		1e	2	95/5	98	96 (R)
9		1a	24	>99/1	55	73 (+)
10 ^{8c}		1b	6	>99/1	98	79 (+)
11		1e	<1	>99/1	99	99 (+)
12		1a	48	97/3	26	36 (-)
13		1e	24	99/1	90	98 (+)
14		1a	48	>99/1	31	15 (+)
15		1e	24	>99/1	84	92 (+)
16		1a	48	97/3	53	80 (+)
17		1e	24	95/5	85	98 (+)
18		1a	60	97/3	25	3 (-)
19		1e	24	97/3	85	97 (+)
20		1a	60	97/3	21	19 (-)
21		1e	30	97/3	82	97 (+)
22		1e	20	>99/1	92	93 (+)
23		1e	10	50/50	90	79 (+)

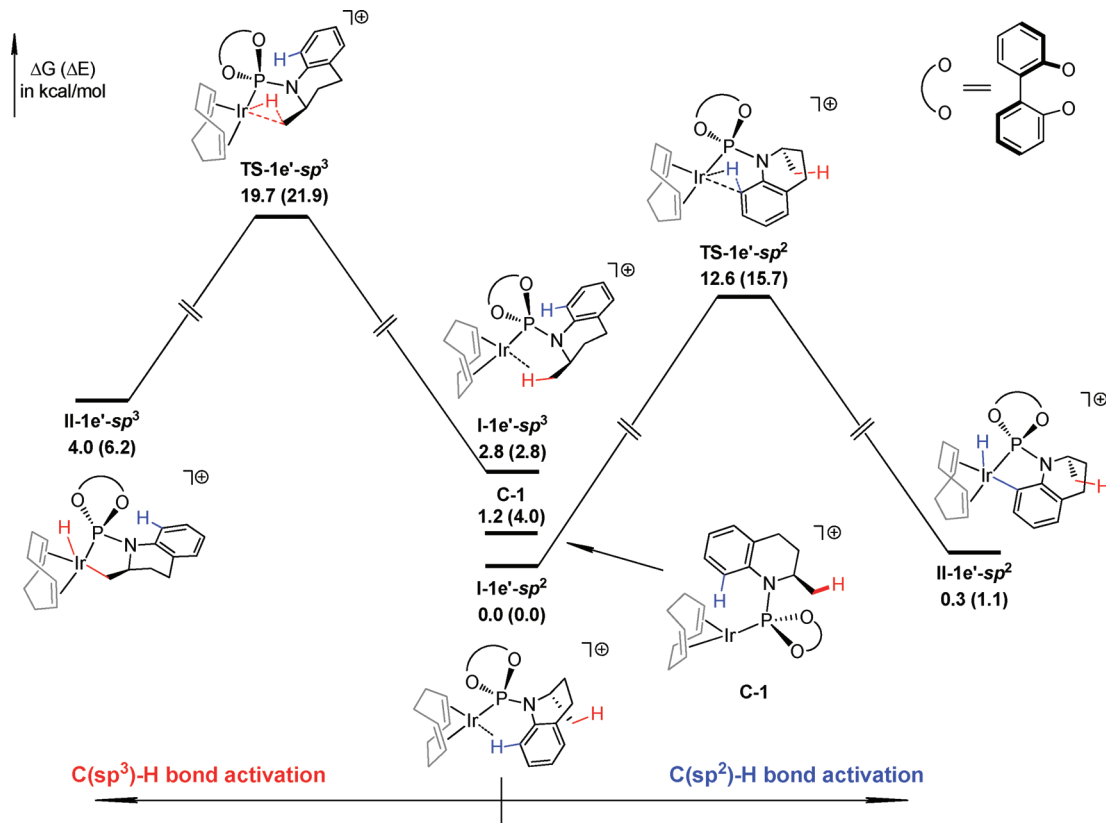
^aThe reactions were conducted under the conditions of entry 8, Table 1.

^bDetermined by ¹H NMR of the crude reaction mixture. ^cIsolated yield of 3 and 4. ^dThe ee was determined by HPLC analysis, and the absolute configuration (or the sign of optical rotation) is indicated in parentheses.

Heteroaryl allyl carbonate **2j** also reacted smoothly with ligand **1e** to produce **3j** in 92% yield and 93% ee (entry 22). Excellent regioselectivity was obtained in most cases (95/5 → 99/1), except for aliphatic allyl carbonate **2k**, which afforded product **3k** in 90% yield but with a branched to linear ratio of 50/50 (entry 23).

Next our efforts were focused on expanding the reaction scope with various ortho-substituted phenyl allyl carbonates, which in general afford poor enantioselectivity with ligands **1a,b**. With *o*-OMe- and *o*-Me-substituted cinnamyl carbonates, 99% and 98% ee were obtained respectively by utilizing ligand **1e** (entries 11 and 13). In sharp contrast, when ligand **1a** or **1b** was employed, only moderate ee values of 36–79% were obtained (entries 9, 10, and 12). 1-Naphthyl allyl carbonate **2f** gave branched product in 92% ee with **1e**, but in only 15% ee with **1a** (entries 14 and 15). Halogen-containing substrates, allowing versatile subsequent transformations, were also investigated. Allylic carbonates **2g–i**, bearing F, Cl, and Br at the ortho position of the phenyl group, could give products **3g–i** in 97–98% ee with **1e** (entries 17, 19, and 21). However,

Scheme 4. Possible C–H Bond Activation Pathways in the Preparation of the Active Catalytic Species with Model Ligand **1e'** Calculated at the M06-2X/SDD/6-31G(d,p) Level of Theory^a



^aThe ΔG and ΔE values (in parentheses) are in kcal/mol.

these corresponding alkylation products were obtained in only 3–80% ee in the presence of ligand **1a** with much longer reaction time (entries 16–21). In addition to the significant improvement of the enantioselectivity, the yields of the products were increased dramatically by **1e** for many cases, such as *m*-methoxyphenyl (98% vs 58%, entries 7 and 8)-, *o*-methylphenyl (90% vs 26%, entries 12 and 13)-, 1-naphthyl (84% vs 31%, entries 14 and 15)-, 2-chlorophenyl (85% vs 25%, entries 18 and 19)-, and 2-bromophenyl (82% vs 21%, entries 20 and 21)-substituted allyl carbonates. This kind of broad scope tolerating ortho-substituted phenyl allyl carbonates has never been realized before.

Formation of Cyclometalated Ir Complexes. The pioneering work by the Hartwig group disclosed that the active catalyst contains the five-membered cyclometalated iridium complex **K1a**,^{6a} formed by C–H activation at the methyl group of ligand **1a**. A similar C–H activation of $\text{P}(\text{OPh})_3$ was also observed earlier by Helmchen and co-workers.¹⁷ For most of the N-aryl ligands, **1e** as an example, there are two possible sites to form the cyclometalated species **K1e-sp**² and **K1e-sp**³, which could be formed respectively via the cleavage of the C(sp²)–H bond at C8 and the C(sp³)–H bond at the methyl group of the tetrahydroquinoline moiety (Scheme 3).

From the data shown in Table 1, two trends could be extracted. First, the absolute configuration of branched products was principally controlled by the BINOL scaffold, and those obtained with R_a axial chirality ligands **1e,g** are the same as that obtained with S_a ligand **1a**. Second, ligands **1h–j**, containing only potential C(sp²)–H activation sites, gave the R

product in good ee (entries 11–13), but ligands **1k,l**, with only possible C(sp³)–H activation sites, afforded the S product with poor enantioselectivity (entries 14 and 15). These results indicate that the cyclometalation of ligands **1a,e** might occur through different manners. To shed light on the mechanism, computational studies and characterizations of iridium complexes have been carried out.

DFT Calculations. DFT calculations were performed to investigate the chemoselectivity between the C(sp²)–H bond and the C(sp³)–H bond activation in the formation of active catalytic species with the phosphoramidite ligands.¹⁸ In our simplified model system, ligands (R,R_a)-**1e** and (R_a,R_a)-**1a** are replaced by their biphenyl-derived analogues **1e'** and **1a'**. The calculations were conducted with the Gaussian09 package¹⁹ using the M06-2X functional.²⁰ For Ir, the SDD basis sets with the associated effective core potential were employed,²¹ while the standard 6-31G(d,p) basis sets were used for all the other atoms.²² All the structures were optimized in THF ($\epsilon = 7.4257$) with the SMD model.²³ Frequency analyses were conducted to confirm each structure being a minimum (no imaginary frequency) or a transition state (only one imaginary frequency). The gas-phase energies of the intermediates and transition states for the C–H bond activation as well as the allylic complexes with **1e'** are presented in the Supporting Information. The key structural parameters and the energetic trends are similar to those obtained in THF solution. In this article, we mainly discuss the Gibbs free energies in THF (ΔG) unless specified. The electronic energies in THF (ΔE) are also given in parentheses for reference.

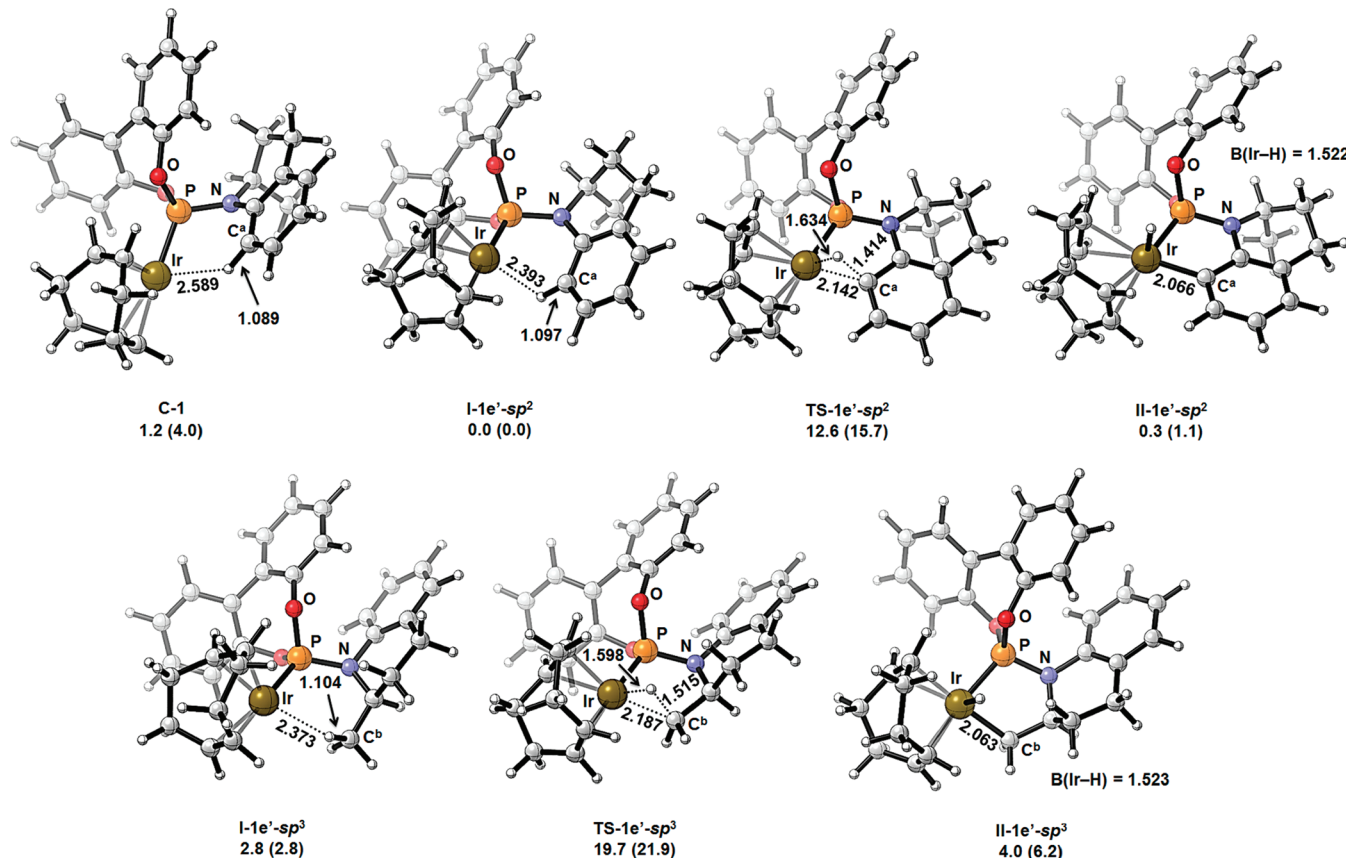


Figure 1. Optimized structures and relative energies of intermediates and transition states for the C–H bond activation with model ligand **1e'**, calculated at the M06-2X/SDD/6-31G(d,p) level of theory. The ΔG and ΔE values (in parentheses) are in kcal/mol. The bond distances are in Å.

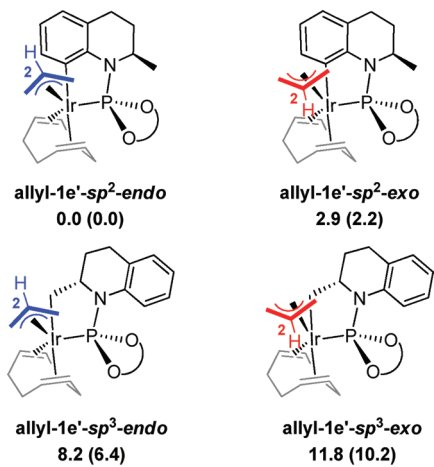
The chemistry of Ir is different from that of Rh, where the chloride is usually still bound to the metal center in the active catalytic species.²⁴ Helmchen and co-workers⁷ showed that adding an Ag(I) salt could facilitate the cyclometalation by chloride abstraction. This method for generation of the active catalytic species was used in the preparation of allyl–Ir complexes with ligand **1e**. The catalysts synthesized in this way exhibit reactivity similar to that obtained *in situ* by procedures A–C in the catalytic reactions described previously (*vide infra*). Therefore, we set the cationic complex **C-1** without a chloride bound to the Ir(I) center as the starting point of the calculation.²⁵ As depicted in Scheme 4 and Figure 1,²⁶ the Ir center in **C-1** has a vacant coordination site; the distance between Ir and the nearest proton on the phenyl ring of the ligand is 2.589 Å. Either the aromatic C(sp²)–H bond or the methyl C(sp³)–H bond of the 2-methyltetrahydroquinoline moiety in **C-1** can interact with the Ir center to form two types of agostic intermediates (**I-1e'-sp²** and **I-1e'-sp³**). **I-1e'-sp²** is the most stabilized isomer and is set as the energy reference. The calculated ΔG values of **C-1** and **I-1e'-sp³** are 1.4 and 2.8 kcal/mol relative to that of **I-1e'-sp²**, respectively. The transition states and the direct products of the following C–H bond cleavage from these agostic intermediates were also located. The energetic barrier of aromatic C(sp²)–H bond activation (**TS-1e'-sp²**) is 12.6 kcal/mol, leading to the Ir–H species **II-1e'-sp²** (0.3 kcal/mol). On the other hand, the methyl C(sp³)–H bond activation has a much higher energetic barrier (**TS-1e'-sp³**, 19.7 kcal/mol) and the Ir–H species generated (**II-1e'-sp³**, 4.0 kcal/mol) is also unstable in comparison to its C(sp²)–H bond activation counterpart.

These results indicate that the aromatic C(sp²)–H bond activation is both kinetically feasible and thermodynamically favored for ligand (R,R_a)-**1e**.

Subsequently, the thermodynamic stabilities of the allylic complexes with different types of metallacycles were compared. In each case (generated via C(sp²)–H bond or C(sp³)–H bond activation), the allylic moiety can adopt two different configurations. We define in this article that the complex with the C2–H bond of the allylic moiety pointing toward the amine part of the ligand as endo, while the complex with the C2–H bond of the allylic moiety pointing toward cod as exo (Scheme 5). The calculation results showed that **allyl-1e'-sp²-endo** is the most stabilized isomer. The relative energy of **allyl-1e'-sp²-exo** is 2.9 kcal/mol. On the other hand, the allyl complexes with the metallacycle derived from the C(sp³)–H bond activation are generally very unstable compared to the C(sp²)–H bond activation counterparts. The relative energies of **allyl-1e'-sp³-endo** and **allyl-1e'-sp³-exo** are 8.2 and 11.8 kcal/mol, respectively.²⁷ These data suggest that the allylic complex with the C(sp²)–H bond activation is the favored intermediate with ligand (R,R_a)-**1e**.

The next question to be addressed is why methyl C(sp³)–H bond activation occurs when Feringa-type ligands are used, since they also have a potential C(sp²)–H bond activation site. Similar calculations were carried out on the simplified Feringa-type ligand **1a'**. As shown in Scheme 6 and Figure 2,²⁶ complex **C-2** is the direct product of chloride abstraction with an Ag(I) salt.²⁵ The Ir center in this complex also has a vacant coordination site. The distance between Ir and the nearest proton on the methyl group of the ligand is 2.522 Å. Different

Scheme 5. Possible (π -Allyl)-Ir Complexes with Model Ligand **1e'** Calculated at the M06-2X/SDD/6-31G(d,p) Level of Theory^a



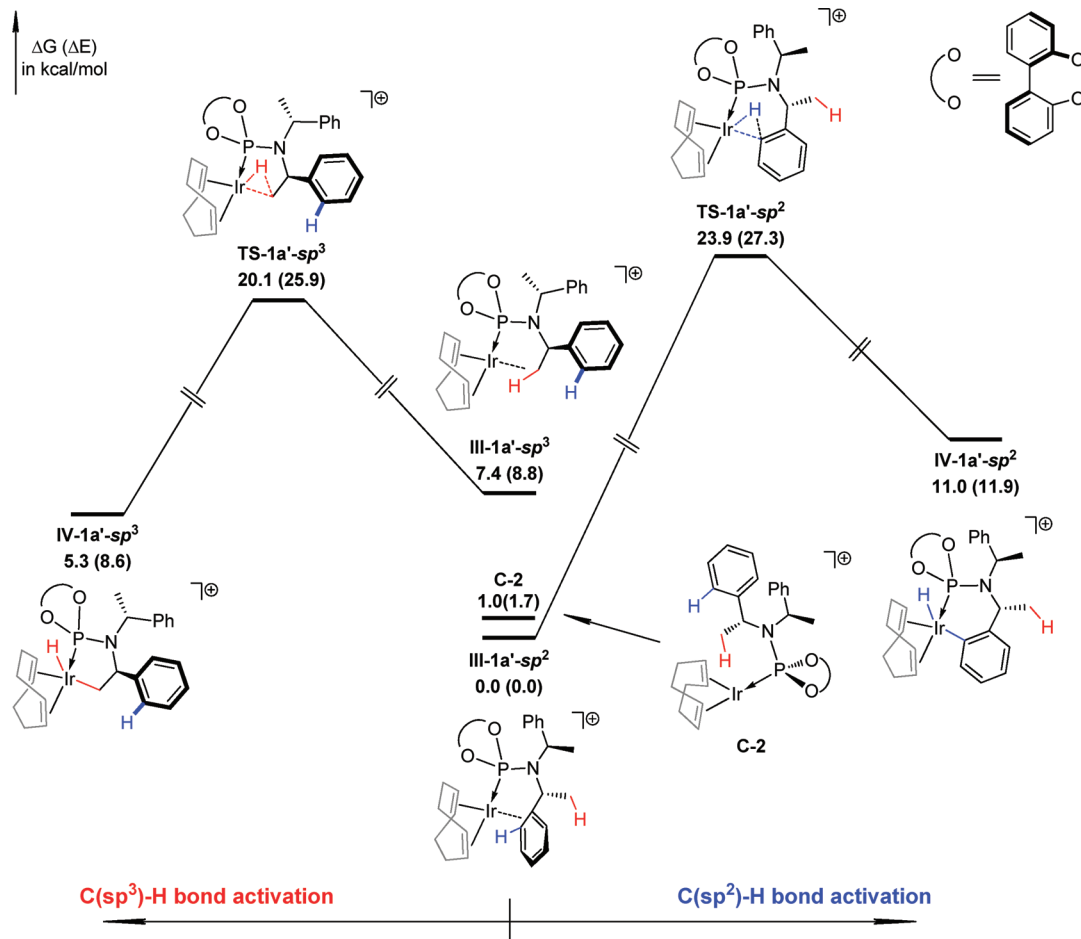
^aThe ΔG and ΔE values (in parentheses) are in kcal/mol.²⁸

from the case for ligand **1e'**, the Ir center in this system is favored to coordinate with the phenyl ring of the chiral amine part rather than either of the C–H bonds to form the stabilized

complex **III-1a'-sp**.²⁹ This complex is set as the energy reference, and the relative energies of **C-2** and the agostic complex (**III-1a'-sp**) in which the Ir center interacts with the methyl C(sp³)–H bond of the ligand are 1.0 and 7.4 kcal/mol, respectively. The transition states and the direct products of the C–H bond cleavage processes were also located. The energetic barrier of the C(sp³)–H bond activation of the phenyl ring (**TS-1a'-sp**) is 20.1 kcal/mol, affording the corresponding Ir–H intermediate **IV-1a'-sp** (5.3 kcal/mol). However, the C(sp²)–H bond activation of ligand **1a'** is less feasible. The ΔG value of **TS-1a'-sp** (23.9 kcal/mol) is higher than that of **TS-1a'-sp** by 3.8 kcal/mol. In addition, the Ir–H intermediate generated through C(sp²)–H bond activation (**IV-1a'-sp**, 11.0 kcal/mol) is also thermodynamically unstable in comparison to **IV-1a'-sp**. These results indicate that the C(sp³)–H bond activation is the favored process with a Feringa-type ligand, which is consistent with the experimental observations.^{6a}

The structures of the (π -allyl)–Ir complexes with different types of metallacycles of ligand **1a'** were also optimized. The relative energy of the (π -allyl)–Ir complex with the metallacycle derived from C(sp²)–H bond activation (**allyl-1a'-sp²-endo**) is 12.5 kcal/mol higher than the C(sp³)–H bond activation counterpart **allyl-1a'-sp³-endo** (Scheme 7), which indicates that the (π -allyl)–Ir complex with the C(sp³)–H bond activation should be the thermodynamically more

Scheme 6. Possible C–H Bond Activation Pathways in the Preparation of the Active Catalytic Species with Model Ligand **1a'** Calculated at the M06-2X/SDD/6-31G(d,p) Level of Theory^a



^aThe ΔG and ΔE values (in parentheses) are in kcal/mol.

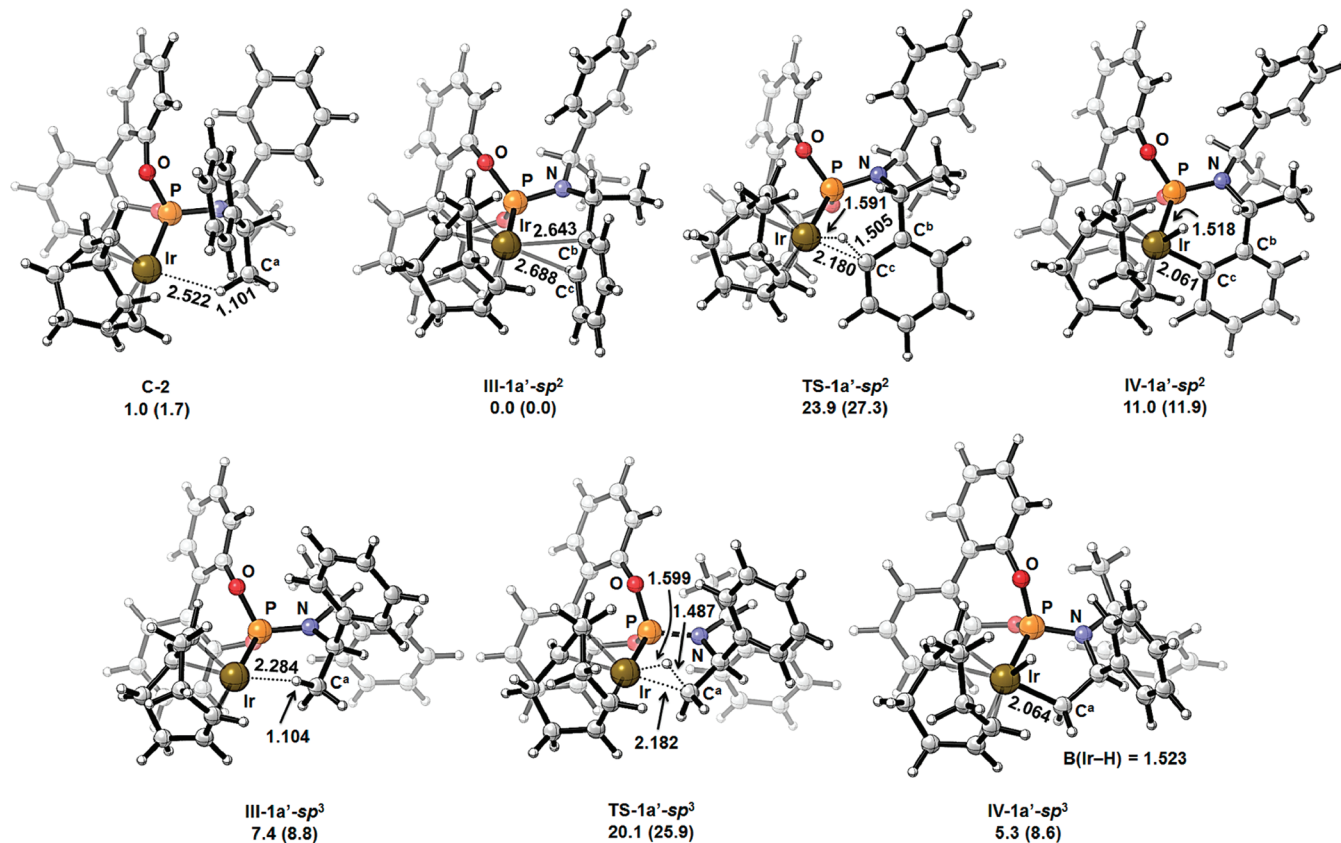
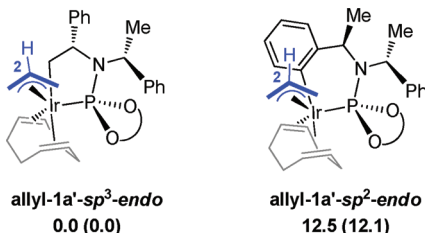


Figure 2. Optimized structures and relative energies of intermediates and transition states for the C–H bond activation with model ligand **1a'**, calculated at the M06-2X/SDD/6-31G(d,p) level of theory. The ΔG and ΔE values (in parentheses) are in kcal/mol. The bond distances are in Å.

Scheme 7. Possible (π -Allyl)–Ir Complexes with Model Ligand **1a' Calculated at the M06-2X/SDD/6-31G(d,p) Level of Theory^a**



^aThe ΔG and ΔE (in parentheses) are in kcal/mol.²⁸

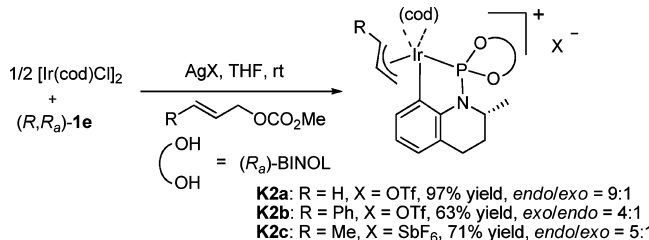
stabilized intermediate for ligand (R,R,R_a) -**1a**. These results are in accord with the single-crystal X-ray diffraction analyses reported by Hartwig^{1c,6b} and Helmchen.⁷

The possible origination leading to such different chemoselectivities with these two systems is summarized as follows. Electronically, the benzene ring in (R,R,R_a) -**1a** is not electron-rich compared to the case for (R,R_a) -**1e**, where the benzene ring is substituted by an N atom. Therefore, the C–H bond activation at the electron-rich aromatic ring through an oxidative addition mechanism should be more favored. In addition, the ring size of the metallacycles also contributes to the selectivity between two C–H bond activation pathways. Both the C(sp²)–H and the C(sp³)–H bond activation of (R,R_a) -**1e** will generate five-membered iridacycles. The C(sp²)–H bond activation should be the kinetically favored process. However, in the case of (R,R,R_a) -**1a** the C(sp²)–H bond activation of the phenyl ring will provide a highly strained

six-membered iridacycle ($A(\text{Ir}-\text{P}-\text{N}) = 119.4^\circ$ in **TS-1a'-sp²**). The C(sp³)–H bond activation of one methyl group affords a more favorable situation ($A(\text{Ir}-\text{P}-\text{N}) = 109.1^\circ$ in **TS-1a'-sp³**), making the formation of a five-membered iridacycle a faster process.

Preparation of the (π -Allyl)–Ir Complexes. To obtain more solid evidence, allyliridium complex **K2a**, cinnamyliridium complex **K2b**, and crotyliridium complex **K2c** were synthesized using a one-pot procedure developed by Helmchen and co-workers (Scheme 8).⁷ These complexes were obtained as

Scheme 8. Synthesis of (π -Allyl)–Ir Complexes **K2a–c**



mixtures of endo and exo isomers, in ratios of 9:1 (**K2a**), 1:4 (**K2b**), and 5:1 (**K2c**), respectively. The crystal structures of these complexes³⁰ clearly show that the metallacycle is formed via C(sp²)–H bond activation^{31,32} of **1e** (Figure 3), which is consistent with the above DFT calculations.

Some selected bond lengths and angles of complexes **K2a–c** are given in Table 3. These complexes can be considered to be severely distorted octahedra with the allyl ligand, an olefinic portion ($\text{C}=\text{C}\text{S}$) of the cod ligand, and the phosphorus

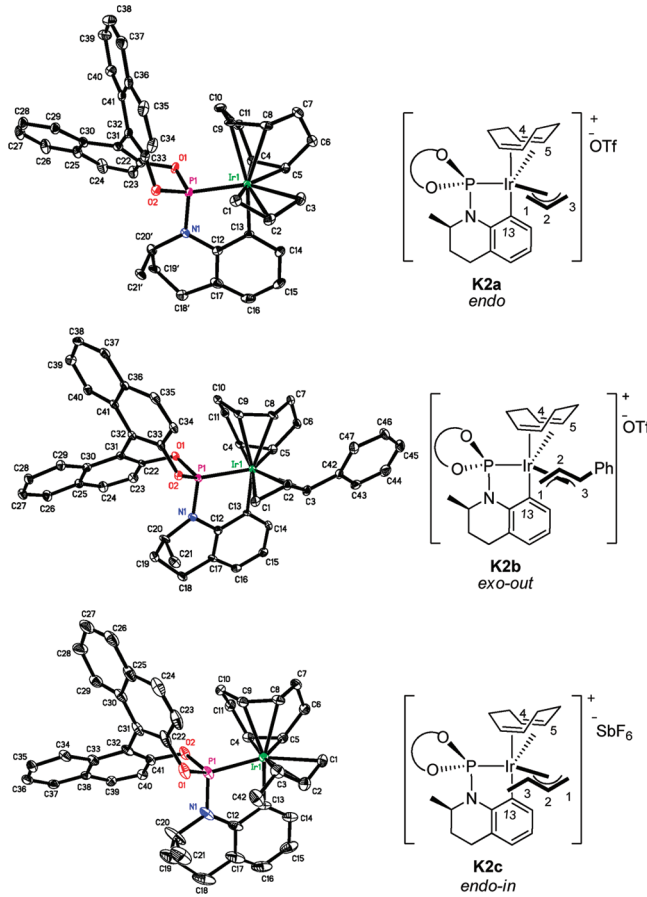


Figure 3. Crystallographic representation of (π -allyl)-Ir complexes K2a–c. Anions and hydrogen atoms are omitted for clarity (ellipsoids are shown at the 30% probability level).

Table 3. Selected Bond Lengths and Bond Angles of (π -Allyl)-Ir Complexes K2a–c

	K2a	K2b	K2c
Bond Lengths (Å)			
Ir–P	2.2733(13)	2.2547(16)	2.268(2)
Ir–C1	2.211(5)	2.227(6)	2.266(7)
Ir–C2	2.210(5)	2.241(6)	2.219(7)
Ir–C3	2.291(5)	2.400(6)	2.267(7)
Ir–C13	2.097(5)	2.101(6)	2.095(7)
C1–C2	1.419(8)	1.414(8)	1.410(12)
C2–C3	1.395(8)	1.392(9)	1.409(12)
Bond Angles (deg)			
P–Ir–C1	88.43(15)	80.30(16)	91.6(2) ^a
C1–Ir–C3	65.9(2)	63.9(2)	65.8(3)
C3–Ir–C5	84.1(2)	89.1(2)	81.6(3) ^b
C5–Ir–C4	36.37(19)	37.0(2)	36.8(3)
C4–Ir–P	87.46(14)	88.20(17)	86.2(2)
sum of Ir–plane	362.06	358.5	362.0
P–Ir–C3	150.38(16)	141.85(16)	153.8(2) ^c
P–Ir–C13	79.82(14)	79.64(16)	79.1(3)
C1–C2–C3	121.1(5)	121.7(6)	121.8(8)

^aThe P–Ir–C3 angle. ^bThe C1–Ir–C5 angle. ^cThe P–Ir–C1 angle.

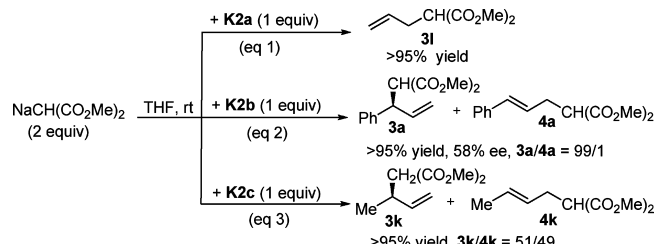
occupying one plane and the other olefinic unit ($C_8=C_9$) of the cod and a phenyl group of the metallacycle lying apical to this plane.^{1c,6b} The summed angles involving the olefinic portion ($C_4=C_5$) of cod, two allyl termini, and the

phosphorus atom of K2a–c are $358.5\text{--}362.1^\circ$, indicating the relative planarity of these groups with the metal. The Ir–C3 bond of K2a is longer than the Ir–C1 bond by 0.08 \AA , likely due to the strong trans influence of the P atom.³³ The C2–H bond of the allyl ligand is pointing away from cod (endo), similar to the case for the Feringa ligand derived complex.^{1c} However, for cinnamyl complex K2b, the C2–H bond is pointing toward cod (exo). The difference between Ir–C3 and Ir–C1 amounts to 0.17 \AA , probably a result of the strong trans influence of the P atom as well as the ability of the phenyl ring to stabilize the neighboring positive charge (see the Supporting Information for the calculated FMOs and NBO charge distribution in the allylic parts of complexes K2a–c). These results suggest that the Ir–C3 bond is weaker and C3 is more electropositive than C1. In addition, the *Re* face of C3 is shielded with the chiral pocket generated by the ligand. Thus, the nucleophile prefers to attack from the *Si* face at C3 to give the *R*-branched product, in accord with the experimental observation. The pocket for the allyl ligand in cinnamyl complex K2b is much larger than that in the Feringa ligand derived complex, which might allow the bulky ortho-substituted cinnamyl derivatives to generally proceed with excellent yield and enantioselectivity (see the Supporting Information for a CPK model of complex K2b).

Interestingly, the crotyl moiety of complex K2c is in the endo-in position, much different from that of K2b. Effected by both the trans P ligand and the methyl substituent, the bond distances of iridium to allyl temini are almost equal. This likely accounts for the poor regioselectivity observed with aliphatic allylic carbonate (entry 23, Table 2).

Reaction of (π -Allyl)–Ir Complexes K2a–c. The stoichiometric reactions of (π -allyl)–Ir complexes K2a–c with sodium dimethyl malonate were studied (Scheme 9).

Scheme 9. Stoichiometric Reactions of (π -Allyl)–Ir Complexes K2a–c



The yields and regioselectivities were comparable to the reactions of corresponding allylic carbonates catalyzed by iridium catalysts prepared in situ. The reaction with 1 equiv of K2b (4:1 exo and endo mixture) afforded 3a in 58% ee, while 50 and 4 mol % of K2b gave the product in 88% and 95% ee, respectively (entry 4 and entry 2, Table 4). The stoichiometric reaction with K2c (5:1 endo and exo mixture) provided 3k in nearly quantitative yield. In general, the π – σ – π transformation of the allyliridium complex is very slow. These data are in agreement with the theoretical results on the assumption that the transformation between the endo and exo forms of the allyl motif is much slower than the nucleophilic attack toward the (π -allyl)–Ir complex. The higher enantioselectivities under catalytic conditions might be explained by the kinetically favorable formation of the exo form of the cinnamyliridium complex that is attacked by the nucleophile before the π – σ – π interconversion.

Table 4. Catalytic Reactions of Cinnamyl Methyl Carbonate **2a** Using (π -Allyl)-Ir Complexes **K2a–c** as Catalysts

entry	K2 (x)	3a/4a	yield (%)	ee (%)
1	K2a (4)	98/2	91	96 (R)
2	K2b (4)	99/1	92	95 (R)
3	K2c (4)	99/1	90	97 (R)
4	K2b (50)	99/1	99	88 (R)

The application of (π -allyl)-Ir complexes **K2a–c** as the catalysts in allylic alkylation reactions with sodium dimethyl malonate is shown in Table 4. With 4 mol % of **K2a–c**, the alkylated products were obtained in 90–92% yield with 95–97% ee and up to 99:1 branched to linear ratio (entries 1–3, Table 4). The absolute configuration of the branched product obtained here is also the same with that obtained with *in situ* prepared catalyst. These results support that the (π -allyl)-Ir complexes are intermediates of the catalytic cycle.

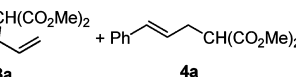
CONCLUSION

In summary, a series of N-aryl phosphoramidites has been synthesized and applied in Ir-catalyzed asymmetric allylic alkylation reactions. The reactions employing these ligands feature broad substrate scope. Excellent regio- and enantioselectivities could be achieved for ortho-substituted phenyl allylic substrates. Mechanistically, the active iridium catalysts derived from the phosphoramidite ligand **1e** are formed by a $C(sp^2)$ –H activation of the N-aryl group in the ligands. The DFT calculations and X-ray crystallographic analyses of the (π -allyl)-Ir complexes explain and support this $C(sp^2)$ –H activation mode and the excellent selectivities obtained in the allylic alkylation reactions. The studies here highly broaden the substrate scope in Ir-catalyzed allylic substitution reactions and provide a better understanding of the reaction mechanism as well as a basis for future ligand design.

EXPERIMENTAL SECTION

General Procedure for Ir-Catalyzed Allylic Alkylation (Entry 8, Table 1). In a dry Schlenk tube filled with argon, $[Ir(cod)Cl]_2$ (3.3 mg, 0.005 mmol, 2 mol %), phosphoramidite ligand **1e** (4.6 mg, 0.01 mmol, 4 mol %), and *n*-propylamine (0.3 mL) were dissolved in THF (0.5 mL). The reaction mixture was heated at 50 °C for 30 min, and then the volatile solvents were removed under vacuum to give a yellow solid. In this tube, allylic carbonate **2a** (0.25 mmol), THF (1.5 mL), and sodium dimethyl malonate solution (0.5 mmol in 1.0 mL THF, 2 equiv) were added and stirred at room temperature until the reaction was complete. The reaction was quenched by saturated aqueous NH_4Cl (2 mL) and extracted with Et_2O (5 mL \times 3). The combined organic layer was washed with brine, separated, and dried over anhydrous Na_2SO_4 . The solvent was evaporated, and the ratio of regioisomers (branched to linear b:l) was determined by 1H NMR of the crude reaction mixture. The residue was purified by silica gel column chromatography using 10/1 PE/EA as the eluent to give the desired product **3a**.

General Procedure for the Preparation of (π -Allyl)-Ir Complexes **K2 (K2a).** A solution of $[Ir(cod)Cl]_2$ (335.5 mg, 0.5 mmol) and ligand **1e** (464.1 mg, 1.0 mmol) in dry THF (10 mL) was added to a flame-dried Schlenk tube under an argon atmosphere. After the mixture was stirred for 30 min at room temperature, $AgOTf$ (258.2 mg, 1.0 mmol) and allyl methyl carbonate (220.5 mg, 3.8 mmol) were added subsequently and the reaction mixture was stirred overnight to give a pale suspension. The precipitate was filtered, and the filtrate was removed under reduced pressure. The residue was washed with Et_2O



(3 mL \times 3) to afford (π -allyl)-Ir complex **K2a** (922.5 mg, 97% yield) as a pale yellow powder, existing as two isomers in a ratio of 9:1. Full details may be found in the Supporting Information.

ASSOCIATED CONTENT

Supporting Information

Text, figures, tables, and CIF files giving experimental procedures, compound characterization data, crystallographic data for the ligands and iridium complexes, and computational details. This material is available free of charge via the Internet at <http://pubs.acs.org>.

AUTHOR INFORMATION

Corresponding Author

*E-mail: slyou@sioc.ac.cn.

Notes

The authors declare no competing financial interest.

ACKNOWLEDGMENTS

The National Basic Research Program of China (973 Program 2009CB825300) and the National Natural Science Foundation of China (Nos. 21121062, 20923005, 20932008, 21025209) are acknowledged for generous financial support. We are also grateful to Prof. Günter Helmchen for helpful discussion, Prof. Xuebing Leng for assistance with X-ray crystallographic analyses, and Prof. Yong-Gui Zhou and Prof. Qinhua Fan for providing the chiral amines.

REFERENCES

- (1) For recent reviews: (a) Helmchen, G.; Dahnz, A.; Dübon, P.; Schelwies, M.; Weihofen, R. *Chem. Commun.* **2007**, 675. (b) Helmchen, G. In *Iridium Complexes in Organic Synthesis*; Oro, L. A., Claver, C., Eds.; Wiley-VCH: Weinheim, Germany, 2009; pp 211–250.
- (c) Hartwig, J. F.; Stanley, L. M. *Acc. Chem. Res.* **2010**, 43, 1461.
- (d) Hartwig, J. F.; Pouy, M. J. *Top. Organomet. Chem.* **2011**, 34, 169.
- (e) Liu, W.-B.; Xia, J.-B.; You, S.-L. *Top. Organomet. Chem.* **2012**, 38, 155.
- (2) For the first example: Takeuchi, R.; Kashio, M. *Angew. Chem., Int. Ed. Engl.* **1997**, 36, 263.
- (3) Janssen, J. P.; Helmchen, G. *Tetrahedron Lett.* **1997**, 38, 8025.
- (4) (a) Bartels, B.; Helmchen, G. *Chem. Commun.* **1999**, 741. (b) Ohmura, T.; Hartwig, J. F. *J. Am. Chem. Soc.* **2002**, 124, 15164. (c) Bartels, B.; Garcia, Y. C.; Helmchen, G. *Eur. J. Org. Chem.* **2003**, 1097. (d) Tissot-Croset, K.; Polet, D.; Alexakis, A. *Angew. Chem., Int. Ed.* **2004**, 43, 2426. (e) Lipowsky, G.; Miller, N.; Helmchen, G. *Angew. Chem., Int. Ed.* **2004**, 43, 4595. (f) Leitner, A.; Shekhar, S.; Pouy, M. J.; Hartwig, J. F. *J. Am. Chem. Soc.* **2005**, 127, 15506. (g) Onodera, G.; Watabe, K.; Matsubara, M.; Oda, K.; Kezuka, S.; Takeuchi, R. *Adv. Synth. Catal.* **2008**, 350, 2725. (h) Fuji, K.; Kinoshita, N.; Tanaka, K.; Kawabata, T. *Chem. Commun.* **1999**, 2289. (i) Fischer, C.; Defieber, C.; Suzuki, T.; Carreira, E. M. *J. Am. Chem. Soc.* **2004**, 126, 1628. (j) Defieber, C.; Ariger, M. A.; Moriel, P.; Carreira, E. M. *Angew. Chem., Int. Ed.* **2007**, 46, 3139. (k) Roggen, M.; Carreira, E. M. *J. Am. Chem. Soc.* **2010**, 132, 11917. (l) Miyabe, H.; Matsumura, A;

- Moriyama, K.; Takemoto, Y. *Org. Lett.* **2004**, *6*, 4631. (m) Nemoto, T.; Sakamoto, T.; Fukuyama, T.; Hamada, Y. *Tetrahedron Lett.* **2007**, *48*, 4977. (n) Kimura, M.; Uozumi, Y. *J. Org. Chem.* **2007**, *72*, 707.
- (5) For a review: Teichert, J. F.; Feringa, B. L. *Angew. Chem., Int. Ed.* **2010**, *49*, 2486.
- (6) (a) Kiener, C. A.; Shu, C.; Incarvito, C. D.; Hartwig, J. F. *J. Am. Chem. Soc.* **2003**, *125*, 14272. (b) Madrahimov, S. T.; Markovic, D.; Hartwig, J. F. *J. Am. Chem. Soc.* **2009**, *131*, 7228.
- (7) (a) Spiess, S.; Raskatov, J. A.; Gnamm, C.; Brödner, K.; Helmchen, G. *Chem. Eur. J.* **2009**, *15*, 11087. (b) Raskatov, J. A.; Spiess, S.; Gnamm, C.; Brödner, K.; Rominger, F.; Helmchen, G. *Chem. Eur. J.* **2010**, *16*, 6601.
- (8) (a) López, F.; Ohmura, T.; Hartwig, J. F. *J. Am. Chem. Soc.* **2003**, *125*, 3426. (b) Shu, C.; Leitner, A.; Hartwig, J. F. *Angew. Chem., Int. Ed.* **2004**, *43*, 4797. (c) Alexakis, A.; Polet, D. *Org. Lett.* **2004**, *6*, 3529. (d) Polet, D.; Alexakis, A.; Tissot-Croset, K.; Corminboeuf, C.; Ditrich, K. *Chem. Eur. J.* **2006**, *12*, 3596. (e) Yamashita, Y.; Gopalarathnam, A.; Hartwig, J. F. *J. Am. Chem. Soc.* **2007**, *129*, 7508. (f) Pouy, M. J.; Leitner, A.; Weix, D. J.; Ueno, S.; Hartwig, J. F. *Org. Lett.* **2007**, *9*, 3949. (g) Liu, W.-B.; He, H.; Dai, L.-X.; You, S.-L. *Org. Lett.* **2008**, *10*, 1815. (h) Liu, W.-B.; Zheng, S.-C.; He, H.; Zhao, X.-M.; Dai, L.-X.; You, S.-L. *Chem. Commun.* **2009**, 6604. (i) Stanley, L. M.; Hartwig, J. F. *J. Am. Chem. Soc.* **2009**, *131*, 8971.
- (9) Liu, W.-B.; He, H.; Dai, L.-X.; You, S.-L. *Synthesis* **2009**, *10*, 2076.
- (10) (a) Wu, Q.-F.; He, H.; Liu, W.-B.; You, S.-L. *J. Am. Chem. Soc.* **2010**, *132*, 11418. (b) Zhuo, C.-X.; Liu, W.-B.; Wu, Q.-F.; You, S.-L. *Chem. Sci.* **2012**, *3*, 205.
- (11) Krasnov, V. P.; Levit, G. L.; Bukrina, I. M.; Andreeva, I. N.; Sadretdinova, L. S.; Korolyova, M. A.; Kodess, M. I.; Charushin, V. N.; Chupakhin, O. N. *Tetrahedron: Asymmetry* **2003**, *14*, 1985.
- (12) (a) Lu, S.-M.; Han, X.-W.; Zhou, Y.-G. *Adv. Synth. Catal.* **2004**, *346*, 909. (b) Lu, S.-M.; Wang, Y.-Q.; Han, X.-W.; Zhou, Y.-G. *Angew. Chem., Int. Ed.* **2006**, *45*, 2260. (c) Wang, Z.-J.; Deng, G.-J.; Li, Y.; He, Y.-M.; Tang, W.-J.; Fan, Q.-H. *Org. Lett.* **2007**, *9*, 1243. (d) Wang, X.-B.; Zhou, Y.-G. *J. Org. Chem.* **2008**, *73*, 5640. (e) Li, Z.-W.; Wang, T.-L.; He, Y.-M.; Wang, Z.-J.; Fan, Q.-H.; Pan, J.; Xu, L.-J. *Org. Lett.* **2008**, *10*, 5265. (f) Zhou, H.; Li, Z.; Wang, Z.; Wang, T.; Xu, L.; He, Y.; Fan, Q.-H.; Pan, J.; Gu, L.; Chan, A. S. C. *Angew. Chem., Int. Ed.* **2008**, *47*, 8464. (g) Gou, F.-R.; Li, W.; Zhang, X. M.; Liang, Y.-M. *Adv. Synth. Catal.* **2010**, *352*, 2441. (h) Zhang, D.-Y.; Wang, D.-S.; Wang, M.-C.; Yu, C.-B.; Gao, K.; Zhou, Y.-G. *Synthesis* **2011**, *12*, 2796.
- (13) (a) Alexakis, A.; Rosset, S.; Allamand, J.; March, S.; Guillen, F.; Benhaim, C. *Synlett* **2001**, 1375–1378. (b) Naasz, R.; Arnold, L. A.; Minnaard, A. J.; Feringa, B. L. *Angew. Chem., Int. Ed.* **2001**, *40*, 927–930. (c) Polet, D.; Alexakis, A. *Synthesis* **2004**, 2586–2590.
- (14) Ligand **1j** has been previously synthesized; see: Toselli, N.; Martin, D.; Achard, M.; Tenaglia, A.; Bürgi, T.; Buono, G. *Adv. Synth. Catal.* **2008**, *350*, 280.
- (15) Isolated yield of single enantiomer after recrystallization of the diastereoisomers; see the Supporting Information for details.
- (16) The structures of **1e,g,k,l** were all confirmed by X-ray crystallographic analyses; see the Supporting Information for details.
- (17) (a) Bedford, R. B.; Castillón, S.; Chaloner, P. A.; Claver, C.; Fernandez, E.; Hitchcock, P. B.; Ruiz, A. *Organometallics* **1996**, *15*, 3990. (b) Bartels, B.; García-Yebra, C.; Rominger, F.; Helmchen, G. *Eur. J. Inorg. Chem.* **2002**, 2569.
- (18) See the Supporting Information for computational details. Helmchen et al. has conducted computational studies on Ir-catalyzed allylic substitution reactions with a Feringa-type ligand.⁷
- (19) Frisch, M. J. et al. *Gaussian09, Revision A.01*; Gaussian, Inc., Wallingford, CT, 2009.
- (20) (a) Zhao, Y.; Truhlar, D. G. *Theor. Chem. Acc.* **2008**, *120*, 215. (b) Zhao, Y.; Truhlar, D. G. *Acc. Chem. Res.* **2008**, *41*, 157.
- (21) (a) Bergner, A.; Dolg, M.; Kuechle, H.; Stoll, H.; Preuss, H. *Mol. Phys.* **1993**, *80*, 1431. (b) Kaupp, M.; Schleyer, P. v. R.; Stoll, H.; Preuss, H. *J. Chem. Phys.* **1991**, *94*, 1360. (c) Dolg, M.; Stoll, H.; Preuss, H.; Pitzer, R. M. *J. Phys. Chem.* **1993**, *97*, 5852.
- (22) (a) Hehre, W. J.; Ditchfield, R.; Pople, J. A. *J. Chem. Phys.* **1972**, *56*, 2257. (b) Hariharan, P.; Pople, J. A. *Theor. Chim. Acta* **1973**, *28*, 213.
- (23) Marenich, A. V.; Cramer, C. J.; Truhlar, D. G. *J. Phys. Chem. B* **2009**, *113*, 6378.
- (24) (a) Yu, Z.-X.; Wender, P. A.; Houk, K. N. *J. Am. Chem. Soc.* **2004**, *126*, 9154. (b) Lee, S. I.; Fukumoto, Y.; Chatani, N. *Chem. Commun.* **2010**, *46*, 3345.
- (25) Chloride anion can readily be abstracted with Ag(I) salt from the neutral Ir(I) complex **L(cod)IrCl**. The calculated Gibbs free energy changes of the chloride-abstraction process are −10.0 kcal/mol (**L = 1e'**) and −12.7 kcal/mol (**L = 1a'**).
- (26) All the figures of the optimized structures in this article were prepared by CYLview: Legault, C. Y. *CYLView, 1.0b*; Université de Sherbrooke, Montreal, Québec, Canada, 2009; <http://www.cylview.org>.
- (27) For a computational study of the stability of π-allyl intermediates in molybdenum-catalyzed asymmetric allylic alkylations, see: Luft, J. A. R.; Yu, Z.-X.; Hughes, D. L.; Lloyd-Jones, G. C.; Krska, S. W.; Houk, K. N. *Tetrahedron: Asymmetry* **2006**, *17*, 716.
- (28) The optimized structures of these complexes are given in the Supporting Information.
- (29) Mezzetti et al. reported an NMR study on the structure of an Ir(I) complex with a Feringa ligand in solution, which showed that the most stable species formed upon chloride abstraction of [Ir(cod)(*R,R,R_a*)-**1a**]Cl is Ir(cod)[(*R,R,R_a*)-**1a**]⁺. These results do not conflict with our calculations because the second molecule of the Feringa ligand should dissociate when the cyclometalation proceeds. Osswald, T.; Rüegger, H.; Mezzetti, A. *Chem. Eur. J.* **2010**, *16*, 1388.
- (30) The racemic iridium complexes **K2a–c** were used for the single-crystal X-ray diffraction analyses; see the Supporting Information for details.
- (31) For the C(sp²)–H activation at Cp*–iridium complexes to form iridacycles, see: (a) Kisenyi, J. M.; Sunley, G. J.; Cabeza, J. A.; Smith, A. J.; Adams, H.; Salt, N. J.; Maitlis, P. M. *J. Chem. Soc., Dalton Trans.* **1987**, 2459. (b) Davies, D. L.; Donald, S. M. A.; Al-Duaib, O.; Macgregor, S. A.; Pölleth, M. *J. Am. Chem. Soc.* **2006**, *128*, 4210. (c) Davies, D. L.; Donald, S. M. A.; Al-Duaib, O.; Fawcett, J.; Little, C.; Macgregor, S. A. *Organometallics* **2006**, *25*, 5976. (d) Li, L.; Brennessel, W. W.; Jones, W. D. *Organometallics* **2009**, *28*, 3492.
- (32) For an enantioselective transfer hydrogenative coupling reaction using a C(sp²)–H activated iridacycle complex as catalyst, see: (a) Kim, I. S.; Ngai, M.-Y.; Krische, M. J. *J. Am. Chem. Soc.* **2008**, *130*, 14891. For a recent review: (b) Hassan, A.; Krische, M. J. *Org. Process Res. Dev.* **2011**, *15*, 1236.
- (33) Appleton, T. G.; Clark, H. C.; Manzer, L. E. *Coord. Chem. Rev.* **1973**, *10*, 335.